SAND2000-1194C

NUMERICAL PREDICTION OF HEAT-FLUX TO MASSIVE CALORIMETERS ENGULFED IN REGULATORY FIRES WITH THE CASK ANALYSIS FIRE ENVIRONMENT (CAFE) MODEL

J. A. Koski, Carlos Lopez
Sandia National Laboratories*
P.O. Box 5800, MS 0718
Albuquerque, NM 87185-0718
(505) 845-9572
Fax: (505) 844-0244
jakoski@sandia.gov

Ahti Suo-Anttila
Innovative Technology Solutions Corporation
6000 Uptown Blvd. N. E., Suite 300
Albuquerque NM, 87110-4162
(505) 872-1089
Fax: 505-872-0233
ajsuoan@swcp.com

M. Alex Kramer, Research Assistant
Miles Greiner, Associate Professor
Mechanical Engineering Department
University of Nevada
Reno, NV 89557
(775) 784-4873
Fax: (775)784-1701
greiner@moriah.ee.unr.edu

ABSTRACT

Recent observations show that the thermal boundary conditions within large-scale fires are significantly affected by the presence of thermally massive objects. These objects cool the soot and gas near their surfaces, and these effects reduce the incoming radiant heat-flux to values lower than the levels expected from simple σT_{fire}^4 models. They also affect the flow and temperature fields in the fire far from their surfaces. The Cask Analysis Fire Environment (CAFE) code has been developed at Sandia National Laboratories to provide an enhanced fire boundary condition for the design of radioactive material packages. CAFE is a set of computer subroutines that use computational fluid mechanics methods to predict convective heat transfer and mixing. It also includes models for fuel and oxygen transport, chemical reaction, and participating-media radiation heat transfer. This code uses two-dimensional computational models so that it has reasonably short turnaround times on standard workstations and is well suited for design and risk studies.

In this paper, CAFE is coupled with a commercial finite-element program to model a large cylindrical calorimeter fully engulfed in a pool fire. The time-dependent heat-flux to the calorimeter and the calorimeter surface temperature are determined for several locations around the calorimeter circumference. The variation of heat-flux with location is determined for calorimeters with different diameters and wall thickness, and the observed effects discussed.

INTRODUCTION

Large packages that transport significant "Type B" quantities of radioactive materials must be qualified to withstand 30 minutes in a fully engulfing pool fire without significant release of contents (see, for example, Title 10, Code of Federal Regulations, Part 71, 1992). Analysis of such fires is complicated by several factors. First, the range of length scales encountered in the physical phenomena is large. For example, turbulence and combustion consist of physical phenomena with scales that range from sub-millimeter to several meters. Secondly, air and thus oxygen are introduced into large pool fires through a complex turbulent mixing process that controls both the location and the intensity of the combustion. Because the fuel-air mixing is limited, combustion temperatures are much lower than the stoichiometric limit. The central region of a pool fire is starved of oxygen, and a vapor dome exists immediately above the pool where evaporated fuel does not have sufficient oxygen to burn. Finally, another strong influence in large open pool fires is the presence of soot particles in the flames. Soot is formed through the inefficient combustion process that is typical of large pool fires. These particles radiate thermal energy with the characteristic orange-yellow glow observed in fires. Experimental evidence of such fire effects is provided in Koski, et al, 1996. Recent studies indicate that the absorption length for thermal radiation in sooty flames is short, on the order of a few centimeters. (Gritzo, et al, 1998).

The focus of the current paper is the evaluation of the fire response of cylindrical objects that are the same size as large transportation casks. Regulations specify that when a physical fire test is performed, the cask must be suspended one meter above a hydrocarbon fuel source and the edges of the fuel region must extend horizontally between one and three meters from the container.

The Cask Analysis Fire Environment (CAFE) computer code (Suo-Anttila, et al, 1999) has been developed to model all relevant fire physics for massive objects engulfed in large fires. It provides a realistic model for use in design of radioactive material packages and in risk-based transportation studies. The CAFE code can be coupled with finite-element models of specific package designs. The coupled system can be used to determine the internal thermal response of engulfed objects to a range of fire environments.

*Sandia is a multi-program laboratory operated by Sandia Corporation, a Lockheed Martin company, for the United States Department of Energy under Contract DE-AC04-94AL85000.

DISCLAIMER

DISCLAIMER

Portions of this document may be illegible in electronic image products. Images are produced from the best available original document.

In this work CAFE is linked to the PATRAN/P-Thermal commercial finite-element program to predict the thermal response of hollow cylindrical test objects to 10CFR71 thermal environments. Four different objects, having two different outer diameters D = 1.22 and 1.82 m (48 and 72 inches) and two different wall thicknesses H = 2.54 and 7.62 cm (1 and 3 inches), are studied. The small and large diameters are roughly the same dimensions as truck and rail transport packages, respectively. Different wall thickness is investigated to determine how the thermal mass of an object affects heat transfer. Many of the effects observed in actual pool fire data are produced.

CAFE MODEL DESCRIPTION

The CAFE code described in Suo-Antilla, et al, 1999 is a complete fire model that includes all of the dominant physics present in fires. CAFE runs rapidly so that it can be used on desktop workstations. It is written in FORTRAN-77 so that it can be compiled on any machine with an F77 compiler. The primary limitation of CAFE is that it is a two-dimensional fire model which applies boundary conditions to three-dimensional objects, although in this paper only two-dimensional objects will be considered. If the object is three-dimensional, the solution is to section the object into multiple two-dimensional cutting planes and the fire model is applied to each of those planes, thus the three-dimensional character of the fire-object interaction can be simulated. Expanding CAFE to a full three-dimensional capability is being considered.

Some of the numerical and physical models included in CAFE are as follows. The governing equations in CAFE are the momentum equations for predicting the velocity field, an energy equation for predicting the temperature field and heat transfer, and three scalar transport equations for tracking the flow of fuel vapor, oxygen and turbulent kinetic energy. CAFE uses the conventional staggered grid finite difference formulation for discretizing the governing equations. In the staggered grid formulation all vector quantities, such as heat-flux and momentum, are defined at the cell interfaces whereas scalar variables, such as temperature and pressure, are defined at cell centers. CAFE uses a variable density variant of the SIMPLE (Patankar and Spalding, 1972) pressure-based solution algorithm to solve the flow equations. Turbulence is modeled by the Prandtl (Schlichting 1979) one equation formulation. Diffusive thermal radiation transport is modeled with the Rosseland approximation. The rate of combustion is modeled by an Arrhenius equation for the reaction rate of fuel and oxygen. The equations are solved in a time stepping procedure so that changes in the flow field and object surface temperature are allowed to interact consistently.

CAFE also uses the Fractional Area Volume Ratio (FAVOR^{TM}) (Sicilian, et. al. 1987) method for representing curved surfaces. The FAVOR^{TM} method allows a diagonal solid surface to appear in a finite-difference computational cell. Thus a curved surface such as a cylinder is represented as a segmented surface. This is a much better representation than a typical stair-step representation that is often used in finite difference codes. A segmented object representation has an equivalent heat transfer and flow representation as a finite-element computational-fluid-dynamics (CFD) method would, yet does not incur the overhead of increased processsor and memory requirements associated with finite-element methods. With the FAVOR^{TM} method the flow areas on all cell surfaces are adjusted to account for the diagonal solid surface. Heat transfer occurs between the gas and solid in the same computational cell through the diagonal surface.

The CFD model in CAFE is coupled to a commercial finite-element code, P-Thermal in this particular case, through a set of user defined subroutines. In principle CAFE can be coupled to any commercial finite-element code that allows users to supply their own subroutines for applying thermal boundary conditions. Surface temperature information of an object is passed from the finite-element model (FEM) by special subroutines to CAFE, which then uses that information to predict a position-dependent heat-flux. The heat-flux is passed back to the FEM which uses the heat-fluxes as local boundary conditions for predicting the object internal thermal response. Thus the FEM has time- and position-dependent fire boundary conditions that depend upon the physics of the problem. The heat-flux and temperature data passing between the CFD and FEM codes is user-controlled. The control logic is based upon the surface temperature rise of the FEM object(s) in the model. The user assigns a minimum temperature rise (5 K was chosen for the problems in this paper). For each FEM time step, the CAFE code checks if any surface node has risen more than the user-assigned value. If the surface temperature change has occurred anywhere on the object(s) then the CAFE CFD model predicts a new distribution of surface heat-fluxes. In generating a surface heat-flux distribution, CAFE integrates its equations of motion and energy forward in time until the new object surface temperature distribution is in quasi-steady equilibrium with the fire.

CAFE COMPUTATIONAL DOMAIN

The computational domain and boundary conditions that are used in CAFE are set up to simulate typical JP4 or JP8 open pool fire conditions. The domain dimensions and boundary conditions for these simulations are depicted in Figure 1. The domain dimensions for the larger and smaller objects are not the same and these dimensions are summarized in Table 1. In Figure 1 the dimension A is the domain width, B is its height, and C is the distance between the bottom of the test object and the bottom of the domain. The dimension E is the width of the region where gas is allowed to escape out of the top of the domain, and W is the width of the fuel pool. The integers N_X and N_Y in Table 1 are the number of elements in the x- and y-directions, respectively.

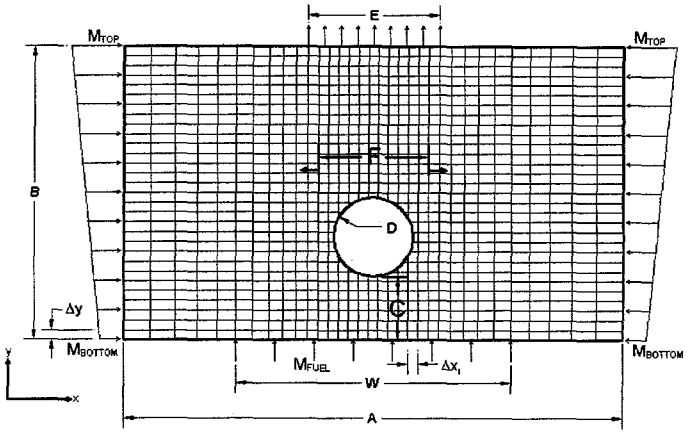

Figure 1. CAFE computational model

The mesh size is not uniform throughout the domain. A variable grid is chosen to enhance the resolution in the regionf the container where square computational cells are chosen and elongated cells appear far from the cylinder. In the central region of width F, the mesh height and width are both Δx_1. Outside this region element-width increases with distance from the fire. The factor a_{XX} is the x-direction-stretching ratio between consecutive elements. The element depth in the direction normal to the page also increases with distance from the fire to account for radial inflow in the z-direction. The factor a_{XZ} is the z-direction extension factor. There was no stretching in the y (vertical) direction in these example problems, though CAFE has the capability to do so. The stretching allows a larger domain to be included in the model without an increased processor overhead. Ideally one would prefer to model a domain of several pool diameters in all directions in order to reduce user-assigned dependencies in the flow-field. However modeling such a large domain would incur an increased processor burden. Instead, carefully assigned boundary conditions are used that mimic the inflow conditions found in a natural open pool fire.

Table 1. CAFE Grid Dimensons and Boundary Conditions

	D=1.22 m (48")	D=1.83 m (72")
A	7.682 m	8.292 m
B	4.575 m	5.185 m
C	1.00 m	1.00 m
E	2.012 m	2.622 m
W	4.218 m	4.828 m
F	1.68 m	2.29 m
$\mathbf{M_{TOP}}$	0.6 kg/m^2	0.6 kg/m^2
$\mathbf{M_{BOTTOM}}$	0.4 kg/m^2	0.4 kg/m^2
$\mathbf{T_{TOP}}$	47°C	47°C
$\mathbf{T_{BOTTOM}}$	27°C	27°C
$\mathbf{T_{FUEL}}$	27°C	27°C
$\mathbf{M_{FUEL}}$	0.08 kg/m^2	0.08 kg/m^2
$\mathbf{Dx_1}$	0.1525 m	0.1525 m
Dy	0.1525 m	0.1525 m
Nx	33	37
Ny	30	34
$\mathbf{a_{xx}}$	9.40%	9.40%
$\mathbf{a_{yy}}$	5.00%	5.00%

A typical open-pool fire has a radial inflow pattern which suggests the use of cylindrical coordinates. However if cylindrical coordinates are used then the round object in the center of the pool would be a sphere rather than a cylinder and that would have the improper surface-to-volume ratio for heat transfer. In order to retain the correct cylinder surface-area and a natural radial-inflow pattern for the outer portions of the fire, a combined radial/Cartesian coordinate system is used. In the region surrounding the central cylinder the computational cells are square with fixed thickness. In regions outside the central object the computational cell is allowed to grow in width as well as thickness. Thus flow from the outer boundaries has a radial inflow character and flow in the region of the central object has a Cartesian character. Although this procedure has user influences, comparisons with open-pool fire data shows that the procedure has merit. If one were to use Cartesian coordinates of fixed thickness throughout the domain the fire structure would be too thin, resulting in flames that barely engulf the object and not consistent with experimental observations.

The inflow velocity at the boundaries is chosen so that the fuel-to-air ratio is approximately 2-4 times stoichiometric in a region two pool-diameters high. This choice comes from the observation that large pool fires have a flaming zone of approximately two pool diameters high. Not all the air that enters the computational grid will be mixed with the fuel; thus the excess air represents the natural updraft that occurs with real fires. If too much excess air is used, the fire puffing will be suppressed which may result in an incorrect heat-transfer distribution. Typical fire puffing is shown in Figure 2. The puffing consists of a horizontal vortex that forms and rises with the flames. The vortex brings in fresh air to the fire at the bottom edge of the vortex and alters the temperature distribution in a transient manner that could not be captured by a steady flow model of a fire. The inlet velocity along both sides of the domain varies linearly from 0.4 m/s at the bottom of the domain to 0.6 m/s at the top. These velocities were chosen to satisfy the requirements mentoned above.

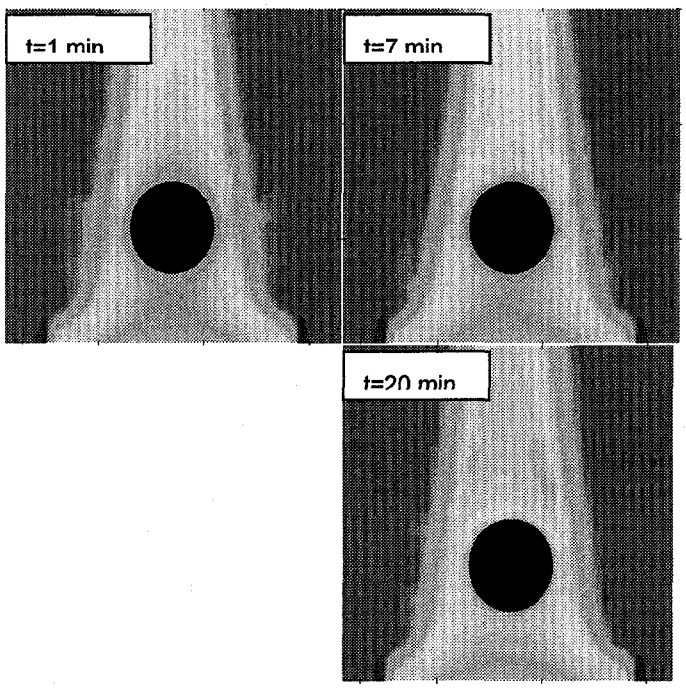

Figure 2. Gray tone temperature plots at times t = 1, 7, 20 minutes. Irregularities at the edges of the fire plume are puffs described in the text.

The exit velocity boundary condition that is applied at the top of the grid is constricted to the central region only. This is because in a real fire the flame velocity is high there. The size of the exit opening is

adjusted so that there is no necking inward or flaring outward of the flames as they exit the computational mesh. In practice, picking the outlet size is a matter of iteration.

Fortunately the heat transfer to the central object is insensitive to the outlet hole size, provided that there is sufficient air inflow. At low inflow conditions a horizontal vortex (which rotates in the opposite direction to the puffing vortices) can form around (or on both sides) of the fire which will capture hot combustion products and artificially increase the fire temperature due to recirculation. A thermally stable temperature stratification of approximately 20°C, with higher temperatures at the top, is included in the inflow air in order to help prevent or reduce vortex formation.

At the bottom boundary a mass flux of pure fuel vapor is injected at a typical open pool evaporation rate of 0.08 Kg/m^2-sec. Typical ranges for open pool evaporation rates vary from 0.04 to 0.08 Kg/m2-sec.

Radiative heat loss from the fire to the environment is not modeled directly in CAFE. Instead the heat of combustion of fuel is adjusted to account for this effect. The justification for this method is that only the outer edges of the fire will react with oxygen and this is where the radiation loss is occurring, thus less net heat is available in the fire for sensible heating of the gas. In addition, incomplete reaction effects, such as soot formation, also reduce the effective heat of combustion of the fuel. A series of test calculations comparing CAFE flame temperatures to measured fire temperatures indicate that an effective heat of combustion of 25MJ/kg leads to good agreement with the experimental data in Koski, 2000 (a typical heat of combustion for hydrocarbon fuels is 42 MJ/kg).

Radiation within the fire is modeled by the Rosseland approximation. This approximation assumes optically thick media and heat transfer is approximated by variable conduction terms in the energy equation. The emissivity of the gas is assumed to be 1 because of the large amount of soot that is present in open pool fuel oil fires. A variable conduction correction is applied at the object surface so that the local cooling effect of the sooty boundary layer near a cool object is accounted for. This correction term can be significant if the computational cells are large and the object is cold, or negligible for small computational cells. Thus the correction term helps to reduce user chosen cell size influences. The object surface emissivity was 0.8 for the problems that appear in this paper.

Four different hollow annular meshes that represent small and large diameter test objects with two different wall thicknesses are constructed using the commercial finite-element code PATRAN. All four models have 40 nodes in the azimuthal direction and 3 elements in the radial direction. The inner surface of the cylinders is insulated. The thermal properties of the test object are those of mild steel.

As indicated in the above discussion of the CAFE model there are a number of assumptions that have been made. The validity of these assumptions will be checked against new experimental data that will be generated during the summer of 2000 at Sandia National Laboratories.

RESULTS

Baseline Geometry Results in this section are for the smaller diameter, smaller thickness object, D = 1.22 m and L = 2.54 cm. In the next section results for larger diameter and thicker wall calorimeters are discussed.

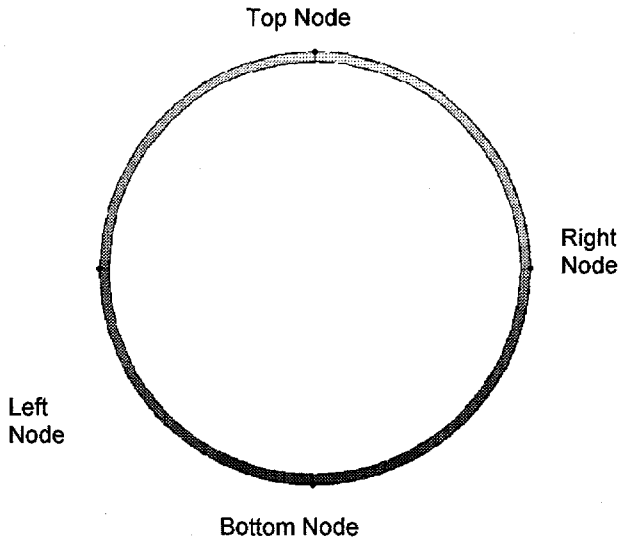

Figure 3. Temperature contour plot of baseline calorimeter after 30 minute fire simulation.

Figure 2 shows three gray-tone temperature contour plots for the fire. These plots are snapshots of the temperature field at times t = 1, 7 and 20 minutes, where t = 0 is the start of the fire simulation. The lightest hues in these figures represent the hottest temperatures. The dark circle suspended in the fire is the round cross section of the calorimeter.

The temperature fields at all three times exhibit a hot fire cone that covers the fuel pool and necks down with increasing elevation. A cool dome is present between the fuel pool and the bottom of the calorimeter in all three figures. This region is oxygen starved (fuel vapor rich). As a result, the rate of combustion is very low and the temperatures are relatively cool. The edges of the hot zones exhibit irregular shapes that are called fire puffs. These puffs form near the bottom of the fire, and they gain elevation and grow with time. These puffs transport air into the hot region of the fire.

At time t = 1 minute the calorimeter is surrounded by a relatively thick cool region as indicated by the gray band around the calorimeter. Even though the fire temperatures are fairly high at this time, the calorimeter is still cool and serves to decrease the temperature of the gas surrounding it. At t = 7 minutes the calorimeter is hotter and the cool boundary layer region has grown thinner, especially at the top. At t = 20 minutes we see that the cool boundary layer is very thin. Moreover, viewing all three figures together, we see that the fire temperatures generally increase with time and the extent of the vapor dome decreases.

Figure 3 is a gray-tone temperature plot of the object at the end of a thirty-minute fire. In this figure, lighter hues again represent higher temperatures. We see that the object temperature is not uniform, but is hottest at the top and coolest at the bottom. The relatively cool vapor dome beneath the object contributes to this temperature stratification. Moreover, the temperature field is nearly symmetric left-to-right. Four nodal locations are also identified at the top, bottom and both sides of the object. The temperature and heat-flux at these locations as functions of time are presented below.

The time-dependent temperatures at the top, side and bottom locations are shown in Figure 4 (the side location represents the average of the left- and right-hand nodes). Note that the vapor dome beneath the calorimeter causes the bottom to be the coolest location throughout the fire period. The side temperature slightly exceeds the top value for the first eight minutes of the fire. After that time, the top of the calorimeter becomes the hottest location on the object. At the end of the thirty minute fire, the temperature at the top of the cask is 1041°C while the temperature at the bottom is 129°C cooler. Finally, all the temperatures are still rising at t = 30 minutes, indicating that the object is not yet in thermal equilibrium with its surroundings.

Marks are placed along the top of Figure. 4 to indicate the times at which CAFE is called by P/Thermal. PATRAN calls CAFE after any temperature in the calorimeter mesh has changed by a specified amount (5°C for these runs). CAFE then runs for a specified flow time (0.5 seconds for these runs) and then it feeds the new heat-flux data back to the P/Thermal routine. Note that CAFE is called very frequently during the first five minutes of the fire. The calls become less frequent at later times after the calorimeter temperature variations become less rapid. The heat-flux predicted by CAFE does depend upon the flow solution of the fire. The more frequently CAFE is called the better the heat-flux prediction. Sensitivity calculations have been performed for the thermal response of the casks as a function of the surface temperature rise parameter. The results indicate that setting a 5 degree temperature rise parameter gives results consistent with results obtained with smaller rise parameters, and use of a smaller parameter would not improve results.

Figure 5 shows the net heat-flux from the fire to the calorimeter versus time and location. These curves are smoothed with eight-point moving averages. The heat-flux at all three locations decreases with time as the temperature of the calorimeter increases. Moreover, the heat-flux is not uniform over the calorimeter surface. For the first 17 minutes of the fire, the bottom heat-flux is the lowest of any location due to its proximity to the relatively large vapor dome. Initially the side heat-flux is the greatest of the three locations. However, after four minutes, the heat-flux at the top becomes the highest. This crossover is caused by the decreasing thickness of the thermal boundary layer at the top of the object, described in connection with Figure. 2. At t = 17 minutes, the net heat-flux at the top and side drop below the flux at the bottom. The decreasing size of the vapor dome causes this. We note, however, that the heat-flux at this time is only one-third of the initial value.

Figure 6 shows the net heat-flux versus surface-temperature boundary conditions at the top, side and bottom locations. These results were obtained by simulating a 60-minute duration fire. This longer duration simulation was required so that all locations on the object reached their steady state temperatures and their net heat-flux rates approached zero.

Note that the heat-flux at all locations decreases as the surface-temperature increases. However, the heat-flux versus surface-temperature boundary condition is not the same at different locations around the cask. The spatial variation of fire temperature and the influence of the cool boundary layer around the object cause this. The heat-flux to the bottom of the object is the smallest of any location for the full range of surface temperatures. For surface temperatures below 400°C (the initial 4 minutes of the fire), the heat-flux to the side is the largest on the object, but the heat-flux to the top is the greatest at higher surface temperatures.

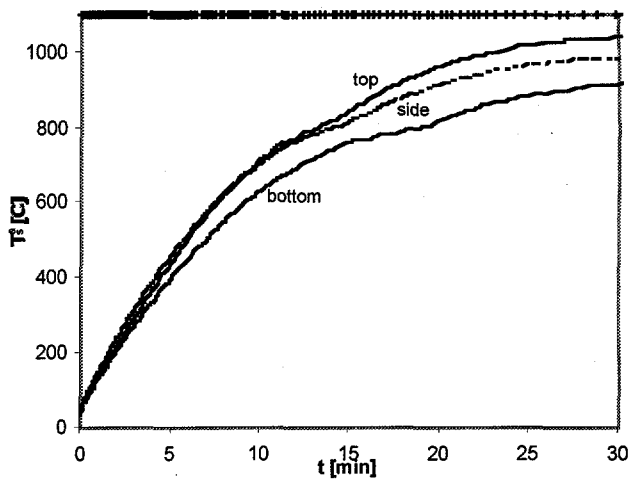

Figure 4. Node temperature versus time for baseline calorimeter. Tick marks at top indicate CAFE clls

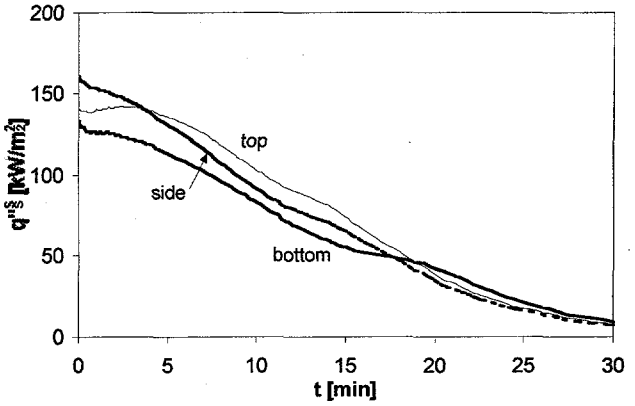

Figure 5. Smoothed heat-flux versus time and location for baseline caolorimeter

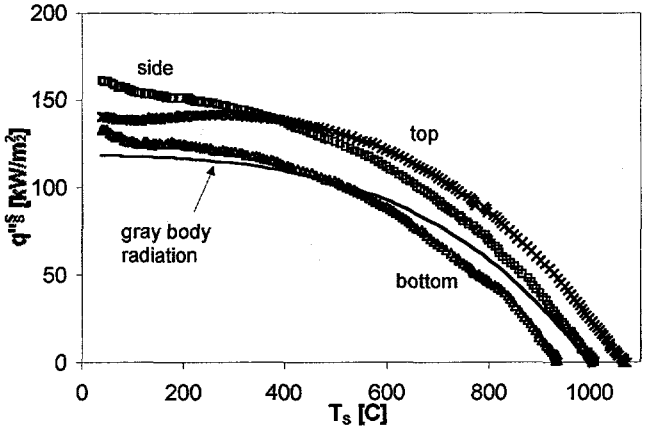

Figure 6. Smoothed heat-flux versus temperature thermal boundary condition for baseline calorimeter

A line is included in Figure 6 that represents gray body radiation heat-flux from a black surrounding at a temperature of $T_{F,e}$ = Figure 2 shows that the fire exhibits large temperature variations from location to location. One measure of an effective-average fire temperature is the average surface-temperature of an engulfed object after it has reached steady state. For the current simulation (and its 1000°C to a body of emissivity $\varepsilon = 0.8$, i.e. q_S"associated assumptions) the effective fire temperature is $T_{F,e} = 1000°C$. $= \sigma\varepsilon(T_S^4 - T_{F,e}^4)$, where σ is the Stefan-Boltzmann constant. We see that the shape of this line is not a good representation of the heat-flux boundary conditions. The reason a single back body temperature is not a good characterization of the heat-flux is due to variations in temperature and geometry of the fire as a function of the cask heating. When the cask is cold, the fire is slightly smaller due to the thinner cool boundary layers surrounding the object. As the object heats up, the fire swells slightly in size and the fire temperature distribution is different. Thus there is no single temperature distribution that will describe the heat transfer in a fire. The effect is non-linear because the cask affects the fire temperature and geometry and that in turn affects the rate and distribution of cask heating.

Geometric Study Figure 7 shows the heat-flux thermal boundary condition at the bottom location for four calorimeters. The letter A is used to represent the baseline geometry with diameter and thickness 1.22 m and 2.54 cm respectively. The other letters represent results for the following pairs of diameter and thickness; B, 1.22 m and 7.64 cm; C, 1.83 m and 2.54 cm; and D, 1.83 m and 7.62 cm. These data are from simulations lasting up to two hours so that the thicker calorimeters could reach their steady state temperature. Arrows are placed on the figure to indicate the conditions at the end of a 30-minute fire for each object. Figures 8 and 9 present similar results for the side and top locations.

Figure 7 shows that the heat-flux, when plotted against the surface temperature boundary condition at the bottom of the object, is nearly independent of object size and thickness. However, the arrows show that at the end of a 30-minute fire, the surfaces of the thinner walled objects are hotter than the corresponding location of the thick objects, and the heat-flux values are lower. This is expected since the thermal response of the thicker casks is significantly slower that that of the thinner objects due to their larger mass per unit surface area. Because all calorimeters are placed 1 m above the pool, fire conditions below the calorimeter should be the similar for all fires, and the resulting heat-fluxes should be independent of calorimeter size at this location.

Figures 8 and 9 show that the heat-flux versus surface temperature boundary condition at the side and top of the object are strongly affected by the object size but is effectively independent of its thickness. We see that for the initial times of the fire, when the surface temperature is below 200°C the heat-flux to the larger diameter object is greater than that to the smaller calorimeter. This trend, however, reverses in the temperature range $200°C < T_S < 800°C$. The heat-flux versus surface temperature boundary condition is independent of object size at higher temperatures where heat-fluxes are lower.

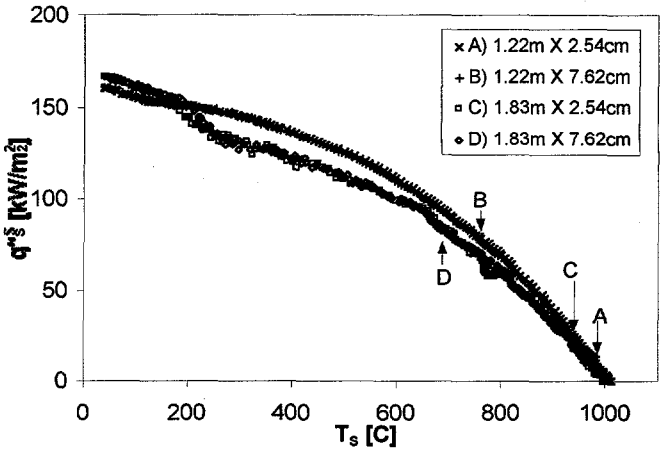

Figure 7. Smoothed heat-flux versus temperature at the bottom of four different calorimgters. Arrows indicate t=30 minutes.

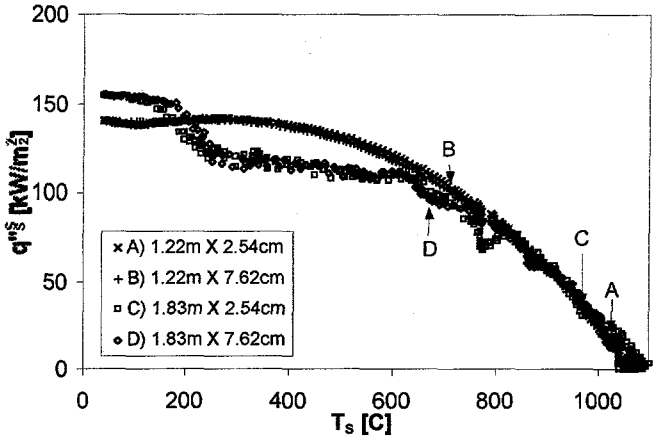

Figure 8. Smoothed heat-flux versus temperature at the sides of four different calorimeters. Arrows indicate t=30minutes.

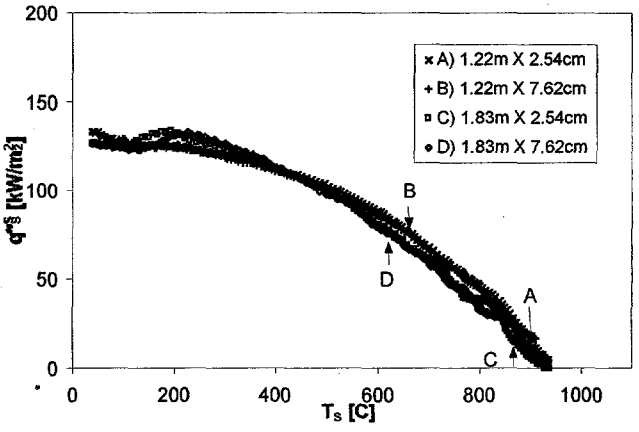

Figure 9. Smoothed heat-flux vs. temperature at the top of four different sized calorimeters. Arrows indicate t=30 minutes.

CONCLUSIONS

Numerical simulations of a large regulatory pool fire have predicted some thermal effects related to cask size and mass. The existence and magnitude of these effects will be confirmed with a fire experiment to be conducted during the summer of 2000 with an instrumented calorimeter of the same cross section as the baseline calorimeter used in this study.

An important prediction of the study is that, while calorimeter diameter affects the heat transfer to the top and sides of the object, different wall thicknesses have the same heat-flux versus surface temperature characteristics. This is seen though the surface temperatures occur later with more massive objects. This effect may be a characteristic of objects with uniform wall thickness, where the heating history is similar, only slower slower thicker walls. The result is not unexpected because the fire model responds to object surface temperatures, not time. Objects with varying wall thickness or containing liquids may respond differently.

The overall heat-flux to the calorimeters was set by setting the heat of combustion of the fuel to a value (25 MJ/kg) that resulted in a distribution of fire temperatures that closely matched existing fire temperature data (Koski, 2000). Calorimeter experiments planned for summer, 2000 in actual pool fires should provide refinements to such results, and provide greater confidence in the model and approach.

References

Gregory, J. J., N. R. Keltner, and R. Mata, Jr. 1989, "Thermal Measurements in Large Pool Fires." *Journal of Heat Transfer* 111, 446-454.

Gritzo, L. A., and V. F. Nicolette. Coupled Thermal Response of Objects and Participating Media in Fires and Large Combustion Systems. in *Heat Transfer in Fire and Combustion Systems*. HTD-Vol. 250. ASME, 1993.

Koski, J. A., 2000, "Measurement of Temperature Distributions in Large Pool Fires with the use of Directional Flame Thermometers," in Proc. 2000 ASME Pressure Vessels and Piping Conference, Seattle WA, July 23-27. (this proceedings).

Koski, J. A. , L. A. Gritzo, L. A. Kent, and S. D. Wix, 1996. Actively Cooled Calorimeter Measurements and Environment Characterization in a Large Pool Fire, *Fire and Materials*, Vol. 20, No. 2, pp 69-78, March-April.

Schlichting, H., 1979, *Boundary Layer Theory,* McGraw-Hill, New York.

Patankar S.V. and Spalding, D. B., 1972, "A Calculational Procedure for Heat Mass and Momentum Transfer in Three Dimensional Parabolic Flows," *Int. J. Heat and Mass Transfer*, Vol. 15, pp. 1787-1806

Sicilian, J. M., Hirt, C. W., Harper, R. P., 1987, "FLOW-3D: Computation Modeling Power for Scientists and Engineers," Flow Science Report FSI-87-00-1, Los Alamos, NM.

Suo-Anttila, A. J., J. A. Koski, and L. A. Gritzo, 2000, CAFE: A Computer Tool for Accurate Simulation of the Regulatory Pool Fire Environment for Type B Packages, in Proc. 1999 ASME Pressure Vessels and Piping Conference, Boston, MA, August 1-5, 1999.

U.S. Nuclear Regulatory Commission, "Packaging and Transportation of Radioactive Material," Rules and Regulations, Title 10, Part 71, *Code of Federal Regulations*, April 30, 1992.